# Targeted Lagrangian sampling of submesoscale dispersion at a coastal frontal zone

K. Schroeder,[1] J. Chiggiato,[2,3] A. C. Haza,[4] A. Griffa,[1,4] T. M. Özgökmen,[4] P. Zanasca,[2] A. Molcard,[5] M. Borghini,[1] P. M. Poulain,[6] R. Gerin,[6] E. Zambianchi,[4,7] P. Falco,[7] and C. Trees[2]

Received 5 April 2012; revised 15 May 2012; accepted 16 May 2012; published 9 June 2012.

[1] The potential impact of rapidly-evolving submesoscale motions on relative dispersion is at the forefront of physical oceanography, posing challenges for both observations and modeling. A persistent coastal front driven by river outflows in the North-Western Mediterranean Sea is targeted by two observational cruises conducted in the summer of 2010. The frontal zone is sampled using drifters launched with a multi-scale strategy consisting of modules of triplets, released on either side of the front by small boats. This experiment is original in that the submesoscale range of 100 m to 1000 m is directly targeted, and the results are expected to provide guidance for practical applications, such as prediction of the initial spreading of pollutants and biogeochemical tracers. The influence of submesoscale motions on relative dispersion is quantified using both particle mean square separation as a function of time, and scale-dependent finite-size Lyapunov exponents (FSLE, $\lambda(\delta)$). Our main finding is the identification of a local dispersion regime with values reaching as high as $\lambda \approx 20$ days$^{-1}$ at drifter pair separation distances of $\delta <$ 100 m. This value is more than an order of magnitude greater than that obtained by drifters in the offshore Ligurian current. The Ligurian Sea circulation is modeled using a fully realistic Regional Ocean Modeling System (ROMS) with 1/60° horizontal resolution. It is found that the numerical model significantly underestimates the relative dispersion at submesoscales, indicating the need for particle dispersion parameterizations for unresolved processes. **Citation:** Schroeder, K., et al. (2012), Targeted Lagrangian sampling of submesoscale dispersion at a coastal frontal zone, *Geophys. Res. Lett.*, *39*, L11608, doi:10.1029/2012GL051879.

## 1. Submesoscale Dispersion Problem

[2] An improved insight in submesoscale processes on lateral scales of 100 m to 10 km and temporal scales ranging from hours to days is important to develop a better understanding of multi-scale interactions and energy balance in the ocean, which might provide insight into the initial spreading of pollutants and biogeochemical tracers. Currently, these processes are not well understood and represent an active research area [*Capet et al.*, 2008; *D'Asaro et al.*, 2011]. This is in part because the submesoscale regime corresponds to a transition from the better studied geostrophic mesoscale to turbulent microscale, in which horizontal stirring and vertical mixing are linked [*Molemaker et al.*, 2005; *McWilliams*, 2008; *Klein and Lapeyre*, 2009]. Submesoscale processes also pose a significant challenge to both observations and modeling in that the interaction of a wide range of spatial and temporal scales must be captured simultaneously.

[3] The primary question of interest here is whether relative dispersion over the submesoscales is locally or non-locally controlled [*Bennett*, 1984]. The non-local regime can be identified through the emergence of exponential growth in time of particle pair separations for scales smaller than the mesoscale radius of deformation. Physically, it corresponds to the case in which the mesoscale field controls the particle/tracer transport. For local dynamics, the relative dispersion is scale-dependent throughout the submesoscale regime, implying that observations and a good understanding of the dynamics of turbulent interactions would be needed to develop models and parameterizations for such motions.

[4] Submesoscale features have been notoriously difficult to observe *in situ*, because it is hard to know where they may occur and they could be intermittent. For instance, episodic forcing events may create suitable conditions for the formation of submesoscale features, while these turbulent features may dissipate after a few days or weeks by forward energy cascade. Mixed layer instabilities are perhaps the best understood form of submesoscale flows [*Boccaletti et al.*, 2007; *Fox-Kemper et al.*, 2008; *Özgökmen et al.*, 2011]. Buoyant coastal fronts that may contain them are usually easy to identify through remote sensing. For these reasons, a persistent upper ocean front created by river outflows was targeted in two observational cruises that took place in the same area six weeks apart from one another. The coastal front was identified first by satellite ocean color images and then more precisely by *in situ* measurements. Lagrangian surface drifters were deployed using a novel multi-scale sampling module. Drifters are the preferred instruments because by following the flow, aliasing errors arising from the rapid evolution of submesoscale features are avoided. For instance, the time dependence of the flow field can make it quite challenging to deconvolute the real signal as measured by ship-board and towed instruments, gliders and

[1]Istituto di Scienze Marine, CNR, La Spezia, Italy.
[2]NATO Undersea Research Center, La Spezia, Italy.
[3]Istituto di Scienze Marine, CNR, Venice, Italy.
[4]Rosenstiel School of Marine and Atmospheric Science, University of Miami, Miami, Florida, USA.
[5]LSEET, Université du Sud Toulon-Var, La Garde, France.
[6]Istituto Nazionale di Oceanografia e di Geofisica Sperimentale, Trieste, Italy.
[7]Dipartimento di Scienze per l'Ambiente, Università degli Studi di Napoli, Naples, Italy.

Corresponding author: T. M. Özgökmen, Rosenstiel School of Marine and Atmospheric Science, University of Miami, 4600 Rickenbacker Cswy., Miami, FL 33149-1098, USA. (tozgokmen@rsmas.miami.edu)

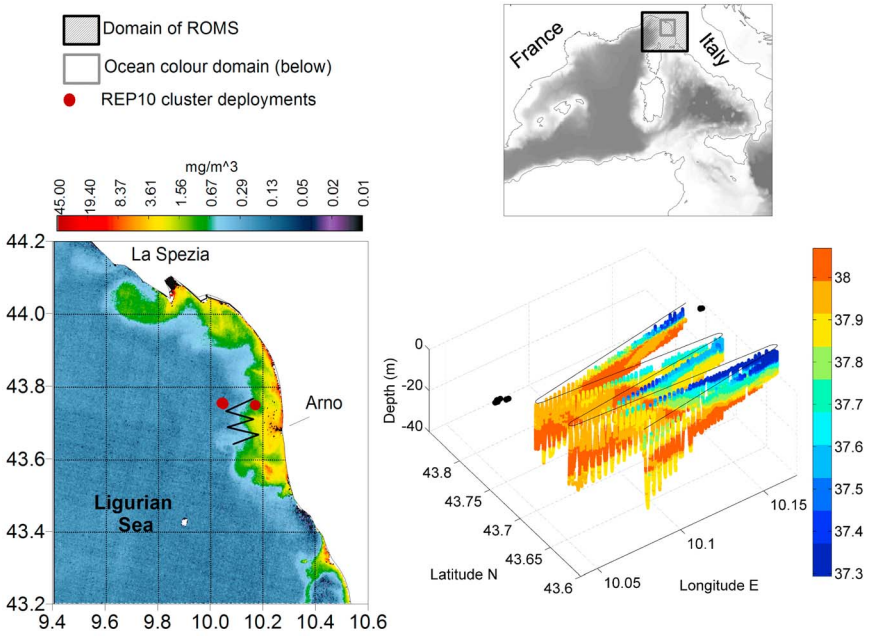


**Figure 1.** (top right) Region of interest, numerical model domain and satellite image frame. (bottom left) Ocean color image (chl1 retrieved from MERIS 09:33 UTC) of 21st August 2010 (before the deployment of the REP10 drifters) with the REP10 cluster deployment positions and the track of the ScanFish MKII used for *in situ* data collection. (bottom right) Vertical salinity section along the ScanFish MKII track with the REP10 cluster deployment positions across the frontal region.

autonomous vehicles. In addition, relative dispersion can be computed on the basis of two-particle statistics. Our main finding is the identification of local dispersion dynamics over the submesoscale flow regime.

## 2. Observational Programs

[5] The area of interest is the Eastern Ligurian Sea (in the North-Western Mediterranean Sea, Figure 1, top right). The region is characterized by depths shallower than 200 m and is influenced by the Arno river discharge [*Ludwig et al.*, 2009] along with some minor rivers, creating favorable conditions for the formation of buoyancy fronts within the coastal area. The Eastern Ligurian Sea is dynamically different from the central and deeper part of the Ligurian basin [*Astraldi et al.*, 1990], which is characterized by a strong and coherent cyclonic circulation (the Liguro-Provencal current), with a typical deformation radius of 10 km or more [*Millot*, 1991]. Relative dispersion in the Liguro-Provencal current was previously studied within the framework of two field experiments (Marine Rapid Environmental Assessment, MREA07/08), where drifters were released in clusters with a separation distance of 1 km [*Schroeder et al.*, 2011]. MREA07/08 results showed the presence of a non-local regime for the submesocale range of 1 to 10 km.

[6] The two experiments reported here took place in the Eastern Ligurian Sea during the summer of 2010 and were conducted by an extensive international partnership. The Ligurian Dispersion Experiment (hereafter LIDEX10) was led by the Italian Consiglio Nazionale delle Ricerche during July 2010 with the RV Maria Grazia, while the Recognized Environmental Picture 2010 experiment (hereafter REP10) was led by the NATO Undersea Research Center with the NRV Alliance during August–September 2010. During both experiments, drifter deployment locations were selected with the help of satellite images, especially the chlorophyll concentration (Figure 1, bottom left) to identify the frontal area separating rich/turbid coastal waters from the offshore waters. In the case of LIDEX10, *in situ* salinity data were collected by performing CTD casts every 0.5 to 1 km across the front (from the surface to a depth of 50 m), while a Scanfish, a towed undulating vehicle, was used to precisely delineate the front during REP10 (Figure 1, bottom right).

[7] The data set used to compute relative dispersion, the primary metric of interest, derive from CODE drifters deployed with a multi-scale approach. The deployment kernel consisted of clusters of nine drifters, composed of three triplets, initially separated by distances ranging between 50 m and 600 m (Figure 2, left). This strategy was chosen to assure that a sufficiently high number of pairs at different separation distances would be available for the computation of dispersion metrics. Nineteen drifters were launched during LIDEX10 and eleven drifters during REP10.

[8] CODE drifters are designed to measure currents within the first meter below the surface [*Poulain*, 1999]. The drifters were equipped with Global Positioning System (GPS) receivers, which has a location accuracy of approximately 10 m, and their position was transmitted every hour. Data were quality controlled, but no filtering was used given our interest in motions at time scales on the order of hours.

[9] While the focus of this study is only on the first days after deployment, the total drifter data from the LIDEX10/REP10 lasted about six months, following similar large-scale pathways documented during MREA07/08 experiments [*Schroeder et al.*, 2011].

## 3. Numerical Modeling

[10] To support the interpretation of the ongoing dynamics, the ocean model ROMS [*Shchepetkin and McWilliams*,

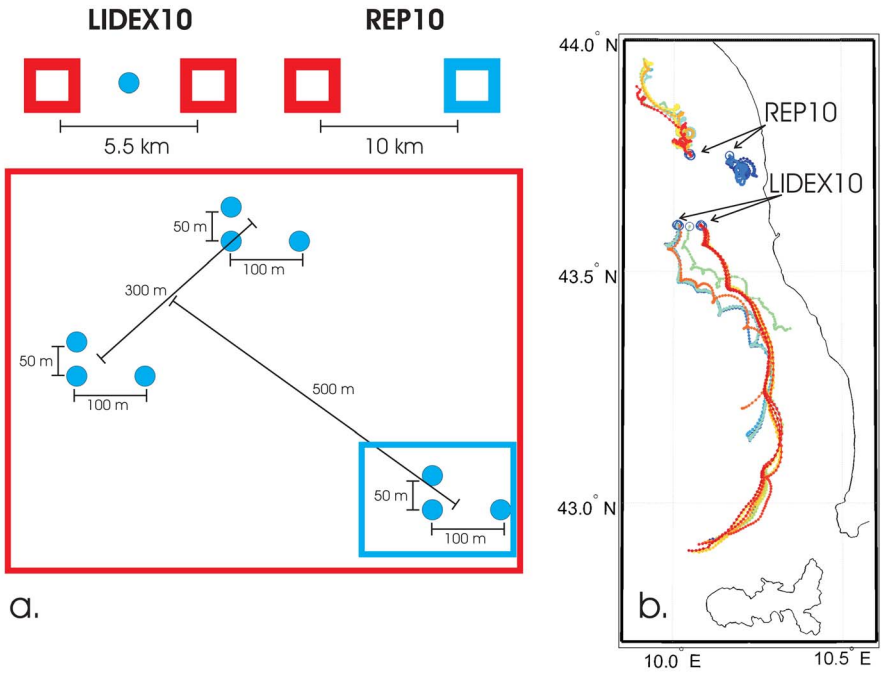


**Figure 2.** (a) Schematic of multi-scale deployment module adopted for the two experiments. During LIDEX10 two clusters consisting of three triplets (red square) were deployed on the two sides of the front at a distance of 5.5 km, with an additional single drifter (light blue circle) launched between them. During REP10 one cluster consisting of three triplets (red square) and one cluster consisting of one triplet (light blue square) were deployed on the two sides of the front at a distance of about 10 km. One of the REP10 drifters was drogued at 15 m, differently from the others, and therefore it was not included in the dispersion analysis. (b) Map showing the drifter trajectories for the first five days after deployment for both experiments.

2005] was employed to simulate the Ligurian Sea circulation during the LIDEX10 and REP10 trials. The horizontal resolution of this model is 1/60°, with 32 vertical $\sigma$-coordinate levels (see Figure 1 for the Ligurian Sea ROMS domain). The model was initialized in May 2010 with the Mediterranean Forecasting System (MFS) model [*Oddo et al.*, 2009] analysis. Open boundary conditions, provided by MFS, were applied to tracers and baroclinic velocity with radiation and nudging [*Marchesiello et al.*, 2001], while free surface and depth-integrated velocity boundary conditions were applied following *Flather* [1976]. The high-resolution, non-hydrostatic, atmospheric model COSMO-ME [*Bonavita and Torrisi*, 2005] of the Italian Air Force National Meteorological Center (Centro Nazionale per la Meteorologia e Climatologia Aeronautica) provided the surface forcing. Three major rivers are included as lateral boundary conditions: Arno (daily discharges, Carlo Brandini personal communication), Serchio and Magra (monthly climatologies). No data assimilation was employed. Additional details on the physics and numerics implemented in this application can be found in *Alvarez et al.* [2012].

[11] To study the dispersion regimes from the ocean model, synthetic drifters were released in the model, following two strategies: (a) Synthetic drifters are launched corresponding to the actual time and location of real deployments LIDEX10 and REP10. (b) In order to ensure statistical reliability of the results, large ensembles of synthetic trajectories are also used for both LIDEX10 and REP10 experiments. The ensembles consisted of 135 particles launched 11 times at 12 hours intervals around the time of actual in-situ drifter deployments. The spatial distribution of each launch consisted of 29 grid points centered around the in-situ drifter launching points, with a cross-configuration corresponding to 1 center particle at each grid point and 4 satellite ones, displaced by 500 m along the four cardinal directions. Drifter trajectories were integrated on-line in 2D at 0.5 m depth in order to mimic the response of the real drifters, and trajectories sampled at 30 minute intervals are used to compute relative dispersion statistics.

## 4. Relative Dispersion From Targeted Launches

[12] Relative dispersion is commonly computed using the mean squared separation of particle pairs, $D^2(t) = \langle |\mathbf{x}^{(1)}(t) - \mathbf{x}^{(2)}(t)|^2 \rangle$, where the superscripts indicate the two particles in each pair and the brackets denote the global average over all pairs. The global averaging operation does not allow for a very systematic investigation of the effects of disparate dynamical scales on the dispersion statistics. Therefore, we also consider the finite-scale Lyapunov exponent, FSLE [*Aurell et al.*, 1997]: $\lambda(\delta) = ln(\alpha)/\langle \tau(\delta) \rangle$, where $\langle \tau(\delta) \rangle$ is the average time required for particle pairs to separate from an initial distance of $\delta$ to $\alpha\delta$. The parameter $\alpha$ is taken as $\alpha = 1.2$ and results are plotted only for pair numbers larger than ten. As in *Schroeder et al.* [2011], the fastest-crossing method is used to compute the FSLE. The reader is referred to *Haza et al.* [2008] and *Poje et al.* [2010] for a multitude of sensitivity tests regarding the computation of $\lambda(\delta)$ from models and ocean data. The Richardson's regime [*Richardson*, 1926] corresponds to $D^2 \sim t^3$ and $\lambda(\delta) \sim \delta^{-2/3}$, the ballistic regime to $D^2 \sim t^2$ and $\lambda(\delta) \sim \delta^{-1}$, and the diffusive regime to $D^2 \sim t$ and $\lambda(\delta) \sim \delta^{-2}$ [*Boffetta et al.*, 2000].

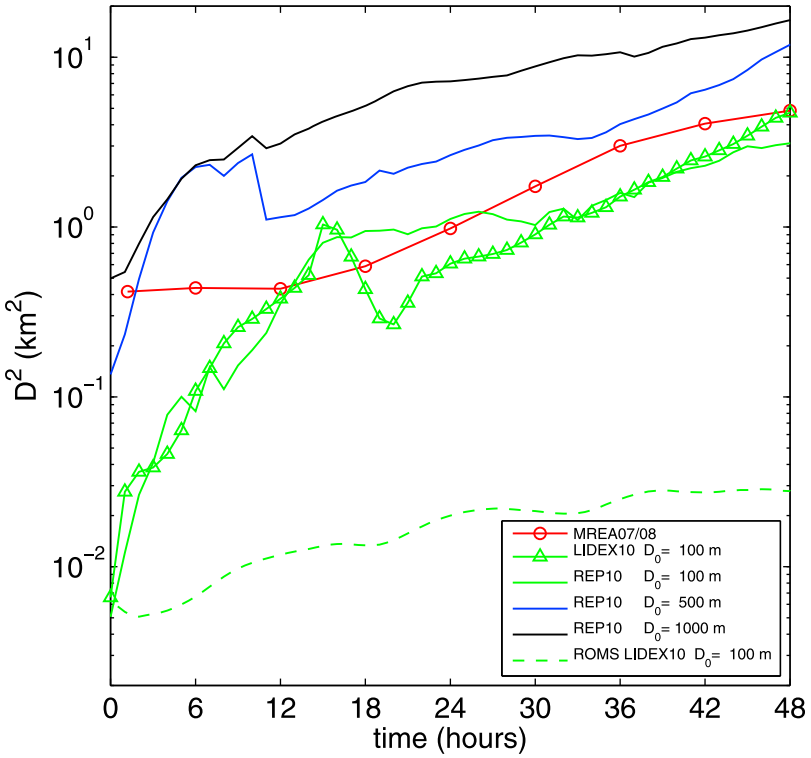


**Figure 3.** Mean square particle separation $D^2(t)$ for various initial distances $D_0$ in a semi-log plot. $D_0$ = 100 m for LIDEX10, and REP10 with $D_0$ = 100 m, $D_0$ = 500 m and $D_0$ = 1000 m. Averaged $D^2(t)$ from MREA07/08 from *Schroeder et al.* [2011] and ROMS results with 19 synthetic drifters launched as in the LIDEX10 are also shown.

### 4.1. Relative Dispersion From Mean Square Particle Separation

[13] It is found that $D^2(t)$ tends to be influenced by specific events governing the flow at the time when drifters are released, thus creating a bias towards the initial state. In order to minimize this dependency, $D^2(t)$ is computed considering both the original and chance pairs. In addition, different values of the initial particle pair separation distance $D_0$ are considered, ranging from 100 m to 1 km. Plots of $D^2(t)$ for 48 hours are shown in Figure 3 with $D_0$ = 100 m for LIDEX10, and with $D_0$ = 100 m, $D_0$ = 500 m, and $D_0$ = 1000 m for REP10. We included $D^2(t)$ from the MREA07/08 data as well for comparison among these different-scale experiments in the nearby regions.

[14] $D^2(t)$ with $D_0$ = 100 m is computed using 64 particle pairs for LIDEX10 and 18 for REP10. The general behavior of LIDEX10 and REP10 appear qualitatively similar, with the primary difference between them being the presence of a peak at around $15 \le t \le 16$ hours with a relative trough at $18 \le t \le 20$ hours in LIDEX10. This peak could be related to the occurrence of a specific event during the first day of LIDEX10, possibly due to a local wind effect or frontal instability inducing flow convergence. The general behavior of LIDEX10 and REP10 can be characterized by a phase of enhanced dispersion during the first $t \approx 15$ hours, and up to separation scales of 1 km. A clear regime change follows with a second phase characterized by slower growth for the following 10 days (only partially shown, since we are focussing on short time scales). During the first phase, the rms particle distance increases from approximately 100 m to 1 km, and the $D^2(t)$ growth deviates from a straight line, which would indicate an exponential behavior on a semi-log plot. This suggests that relative dispersion in the submesoscale range between 100 m and 1 km is likely to be governed by local dynamics, with enhanced dispersion created by submesoscale phenomena active in the buoyant front.

[15] Results using $D_0$ = 500 m and $D_0$ = 1000 m in REP10 also indicate enhanced dispersion regime during the first few hours and up to scales of a several km with the existence of a slower second phase, at scales larger than several km.

[16] It is interesting to compare these results with those from MREA07/08 that were obtained in the highly energetic Liguro-Provencal current. Since MREA07/08 drifters were launched in clusters of a typical size of ≈ 1 km, dispersion at smaller separation scales is not available. The MREA07/08 growth rate appears to be qualitatively similar to that during the second phase observed in REP10 and LIDEX10, occurring at separation scales greater than 1 km and periods longer than a day. Our dedicated launch strategy to sample the submesoscale separation scales in LIDEX10 and REP10 certainly seems to present an advantage with respect to that in MREA07/08. But there seems to still be a considerable difference between the coastal and open ocean settings in that the initial enhanced dispersion regime is not observed in the MREA07/08 data.

[17] Finally, 19 synthetic drifters launched in ROMS as in LIDEX10 are seen to result in a significant underestimation of dispersion over the 48 hour period.

### 4.2. Relative Dispersion From Scale Dependent FSLE

[18] The scale dependent FSLE highlights relative dispersion over the submesoscales. Results from LIDEX10 and

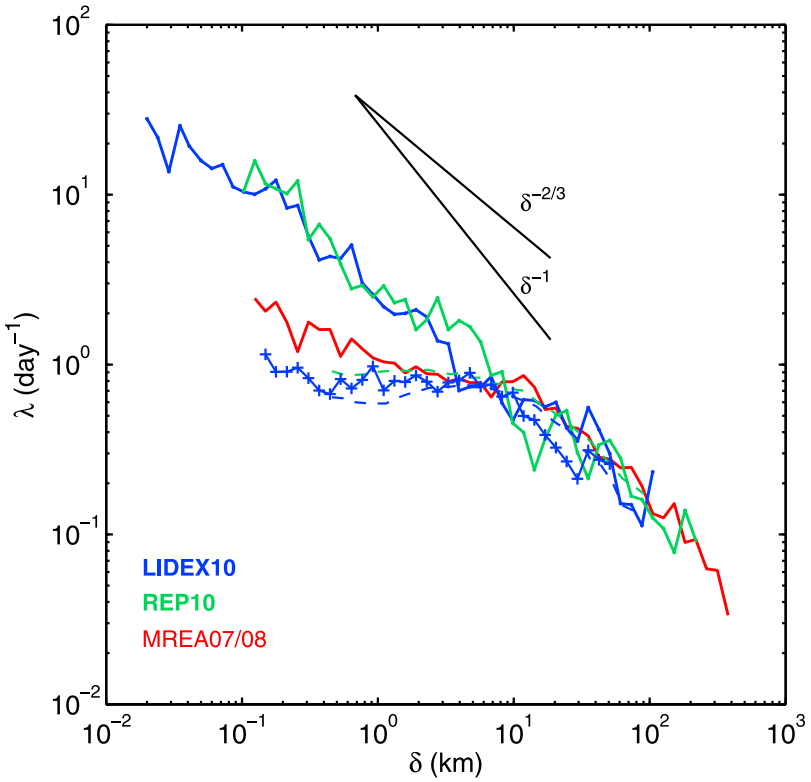


**Figure 4.** Scale dependent FSLE $\lambda(\delta)$ for LIDEX10 (solid blue), REP10 (solid green), and MREA07/08 (solid red). Modeling results from synthetic drifters in ROMS simulations are shown as follows: 19 drifters launched as in the LIDEX10 (blue with "+", strategy-a), 1485 drifters during LIDEX10 (dashed blue, strategy-b) and 1485 drifters during REP10 (dashed green). Ballistic ($\lambda \sim \delta^{-1}$) and Richardson ($\lambda \sim \delta^{-2/3}$) regimes are indicated.

REP10 are presented in Figure 4 and clearly demonstrate a dispersion regime that is scale-dependent (local) at all separation scales. Results from both LIDEX10 and REP10 data are consistent with one another. MREA07/08 results ranging down to $\delta \approx 100$ m are also shown, on the basis of chance pairs. The contrast with respect to MREA07/08 is quite significant over the submesoscales in that there is a persistent increase in the FSLE with a Richardson's power law of $\lambda \sim \delta^{-2/3}$ over the submesoscales ($\delta < 10$ km) ending up with a limiting value of $\lambda_{max} \approx 20$ days$^{-1}$ at the smallest separations of $\delta < 100$ m attained during LIDEX10 and REP10. This value of $\lambda$ is about an order of magnitude greater than that obtained in the Ligurian Sea circulation during MREA07/08. ROMS simulations clearly lack any dispersive turbulent motions below the mesoscale separations of $\delta \leq 10$ km. There is however very good agreement between results from launches with strategy-(a) and strategy-(b) for LIDEX10 over the submesoscales (same for REP10, not shown). Note that all curves converge over the mesoscale regime of $\delta > 10$ km and show ballistic scaling $\lambda \sim \delta^{-1}$, associated with horizontal shear zones created by gyres and boundary currents in the Ligurian Sea.

## 5. Conclusions

[19] Relative dispersion at oceanic submesoscales is still largely unknown, and has been experimentally investigated so far mostly in the open ocean and for scales greater than 1 km [*LaCasce and Ohlmann*, 2003; *Koszalka et al.*, 2009; *Lumpkin and Elipot*, 2010; *Schroeder et al.*, 2011; *Berti et al.*, 2011]. Presented here are results from experiments which directly target relative dispersion induced by a persistent coastal front in the submesoscale range of 100 m to 1000 m. The novel sampling strategy and resulting dispersion curves are expected to provide insight into the quantification of initial tracer dispersion under submesoscale motions.

[20] It is concluded that tightly-spaced clusters of drifters constitute an efficient and inexpensive observational technique to obtain relative dispersion statistics from rapidly-evolving submesoscale flows with minimal aliasing. It is found on the basis of both $D^2(t)$ and $\lambda(\delta)$ that time scales of $t < 15$ hours and space scales of $\delta < 1$ km, that are characteristic of submesoscale phenomena, exhibit enhanced relative dispersion compared to larger scales of motion. In particular, values were obtained reaching $\lambda \approx 20$ days$^{-1}$ for $\delta < 100$ m, which is an order of magnitude greater than those obtained for the off-shore mesoscale flows. Computations with realistically-configured 1/60° ROMS were unable to capture this enhanced dispersion regime, indicating the need for subgrid-scale models for submesoscale transport. This is of importance in practical problems involving multi-scale interactions in the ocean, such as daily prediction of oil spill transport.

[21] **Acknowledgments.** We are indebted to all personnel oboard the NRV Alliance and RV Marian Grazia without whom the success of the cruises LIDEX10 and REP10 would not have been possible. The data processing activity was partly funded by the MED TOSCA project, co-financed by the European Regional Development Fund. We greatly appreciate the support of the Office of Naval Research (ONR) and National

Science Foundation via grants N00014-09-1-0267 and OCE0850714. We thank all members of the ONR Lateral Mixing and Ocean 3D + 1 teams (http://www.whoi.edu/ocean3dplus1), who have provided guidance through many insightful discussions. This research was made possible in part by a grant from BP/The Gulf of Mexico Research Initiative.

[22] The Editor thanks Joseph LaCasce and an anonymous reviewer for assisting in the evaluation of this paper.

## References

Alvarez, A., J. Chiggiato, and B. Mourre (2012), Robotic characterization of access-restricted marine environments, *IEEE Rob. Autom. Mag.*, in press.

Astraldi, M., G. P. Gasparini, G. M. R. Manzella, and T. S. Hopkins (1990), Temporal variability of currents in the eastern Ligurian Sea, *J. Geophys. Res.*, *95*(C2), 1515–1522.

Aurell, E., G. Boffetta, A. Crisanti, G. Paladin, and A. Vulpiani (1997), Predictability in the large: An extension of the concept of Lyapunov exponent, *J. Phys. A*, *30*, 1–26.

Bennett, A. F. (1984), Relative dispersion—Local and nonlocal dynamics, *J. Atmos. Sci.*, *41*(11), 1881–1886.

Berti, S., F. A. D. Santos, G. Lacorata, and A. Vulpiani (2011), Lagrangian drifter dispersion in the southwestern Atlantic Ocean, *J. Phys. Oceanogr.*, *41*, 1659–1672.

Boccaletti, G., R. Ferrari, and B. Fox-Kemper (2007), Mixed layer instabilities and restratification, *J. Phys. Oceanogr.*, *37*, 2228–2250.

Boffetta, G., A. Celani, M. Cencini, G. Lacorata, and A. Vulpiani (2000), Nonasymptotic properties of transport and mixing, *Chaos*, *1*, 50–60.

Bonavita, M., and L. Torrisi (2005), Impact of a variational objective analysis scheme on a regional area numerical model: The Italian Air Force Weather Service Experience, *Meteorol. Atmos. Phys.*, *88*, 39–52.

Capet, X., J. C. Mcwilliams, M. J. Mokemaker, and A. F. Shchepetkin (2008), Mesoscale to submesoscale transition in the California Current system. Part I: Flow structure, eddy flux, and observational tests, *J. Phys. Oceanogr.*, *38*(1), 29–43.

D'Asaro, E., C. Lee, L. Rainville, R. Harcourt, and L. Thomas (2011), Enhanced turbulence and dissipation at ocean fronts, *Science*, *332*, 318–322.

Flather, R. (1976), A tidal model of the north-west European continental shelf, *Mem. Soc. R. Sci. Liege*, *6*, 141–164.

Fox-Kemper, B., R. Ferrari, and R. Hallberg (2008), Parameterization of mixed-layer eddies. Part I: Theory and diagnosis, *J. Phys. Oceanogr.*, *38*, 1145–1165.

Haza, A. C., A. Poje, T. M. Özgökmen, and P. Martin (2008), Relative dispersion from a high-resolution coastal model of the Adriatic Sea, *Ocean Modell.*, *22*, 48–65.

Klein, P., and G. Lapeyre (2009), The oceanic vertical pump induced by mesoscale and submesoscale turbulence, *Annu. Rev. Mar. Sci.*, *1*, 351–375.

Koszalka, I., J. H. LaCasce, and K. A. Orvik (2009), Relative dispersion statistics in the Nordic Seas, *J. Mar. Res.*, *67*, 411–433.

LaCasce, J. H., and C. Ohlmann (2003), Relative dispersion at the surface of the Gulf of Mexico, *J. Mar. Res.*, *61*(3), 285–312.

Ludwig, W., E. Dumont, M. Meybeck, and S. Heussner (2009), River discharges of water and nutrients to the Mediterranean and Black Sea: Major drivers for ecosystem changes during past and future decades?, *Prog. Oceanogr.*, *80*, 199–217, doi:10.1016/j.pocean.2009.02.001.

Lumpkin, R., and S. Elipot (2010), Surface drifter pair spreading in the North Atlantic, *J. Geophys. Res.*, *115*, C12017, doi:10.1029/2010JC006338.

Marchesiello, P., J. McWilliams, and A. Shchepetkin (2001), Open boundary conditions for long-term integration of regional oceanic models, *Ocean Modell.*, *3*, 1–20.

McWilliams, J. (2008), Fluid dynamics at the margin of rotational control, *Environ. Fluid Mech.*, *8*, 441–449.

Millot, C. (1991), Mesoscale and seasonal variabilities of the circulation in the western Mediterranean, *Dyn. Atmos. Oceans*, *15*, 179–214.

Molemaker, M., J. McWilliams, and I. Yavneh (2005), Baroclinic instability and loss of balance, *J. Phys. Oceanogr.*, *35*, 1505–1517.

Oddo, P., M. Adani, N. Pinardi, C. Fratianni, M. Tonani, and D. Pettenuzzo (2009), A nested Atlantic-Mediterranean Sea general circulation model for operational forecasting, *Ocean Sci.*, *5*, 461–473.

Özgökmen, T., A. Poje, P. Fischer, and A. Haza (2011), Large eddy simulations of mixed layer instabilities and sampling strategies, *Ocean Modell.*, *39*, 311–331.

Poje, A., A. Haza, T. Özgökmen, M. Magaldi, and Z. Garraffo (2010), Resolution dependent relative dispersion statistics in a hierarchy of ocean models, *Ocean Modell.*, *31*, 36–50.

Poulain, P.-M. (1999), Drifter observations of surface circulation in the Adriatic Sea between December 1994 and March 1996, *J. Mar. Syst.*, *20*, 231–253.

Richardson, L. F. (1926), Atmospheric diffusion shown on a distance-neighbour graph, *Proc. R. Soc. London, Ser. A*, *110*(756), 709–737.

Schroeder, K., A. C. Haza, A. Griffa, T. M. Özgökmen, P. Poulain, R. Gerin, G. Peggion, and M. Rixen (2011), Relative dispersion in the liguro-provencal basin: From sub-mesoscale to mesoscale, *Deep Sea Res., Part I*, *58*, 861–882.

Shchepetkin, A. F., and J. C. McWilliams (2005), The regional oceanic modeling system (ROMS): A split-explicit, free-surface, topography-following-coordinate oceanic model, *Ocean Modell.*, *9*, 347–404.